

JAERI - M
89-104

13-POINT THOMSON SCATTERING SYSTEM FOR
JFT-2M PLASMA

August 1989

Toshihiko YAMAUCHI, Richard NEUFELD*
and Toshihide OGAWA

JAERI-Mレポートは、日本原子力研究所が不定期に公開している研究報告書です。
入手の問合せは、日本原子力研究所技術情報部情報資料課（〒319-11 茨城県那珂郡東海村
1-1-1）にお申し込みください。このほか、財団法人原子力弘済会資料センター（〒319-11 茨城
県那珂郡東海村日本原子力研究所内）で複写による実費額をお支払いいただけます。

JAERI-M reports are issued irregularly.

Inquiries about availability of the reports should be addressed to Information Division, Department
of Technical Information, Japan Atomic Energy Research Institute, Tokai-mura, Naka-gun,
Ibaraki-ken 319-11, Japan.

C Japan Atomic Energy Research Institute, 1989

編集兼発行 日本原子力研究所
印刷 山田軽印刷所

13-point Thomson Scattering System for JFT-2M Plasma

Toshihiko YAMAUCHI, Richard NEUFELD^{*} and Toshihide OGAWA

Department of Thermonuclear Fusion Research
Naka Fusion Research Establishment
Japan Atomic Energy Research Institute
Naka-machi, Naka-gun, Ibaraki-ken

(Received July 20, 1989)

A 13-point Thomson scattering system mounted on the JFT-2M tokamak routinely provides reproducible electron temperature and density data. Good performance has been achieved with the help of a large collecting lens (capable of gathering data over a vertical 60-cm long plasma volume), the automatic transfer of data from a 180-channel attenuator into the CPU, the use of high-pass optical filters and a large polarizer plate to reduce stray light, and a better matching of LED calibration signal intensities to those of the scattered signals.

Peaked density profiles are measured in improved L-mode (IL) plasmas, in contrast to those observed during the H-mode phase. IL-mode is caused by the broad and high electron temperature. With pellet injection, peaked density profiles are again observed.

Keywords: Thomson Scattering, Glass Fiber Bundle, JFT-2M, 13-point Measurement, Ruby Laser, Peaked Ne Profile, Broad Te Profile, IL-mode, H-mode

* On leave from Hydro-Quebec Research Institute, Quebec, Canada.

JFT-2Mプラズマ用13点トムソン散乱装置

日本原子力研究所那珂研究所核融合研究部
山内 俊彦・Richard NEUFELD*・小川 俊英

(1989年7月20日受理)

JFT-2Mトカマクに取付けられた13点トムソン散乱装置は、定常的かつ再現性良く電子温度及び密度のデータを供給している。大きな集光レンズ(垂直方向60cm長に渡るプラズマのデータを収集)、180チャンネルの減衰率を計算機メモリへ自動転送、迷光を除去する為に高エネルギー帯を通す光学フィルター及び大偏光板の適用、LED較正信号と散乱信号の対応を良くしたこと等により、良い性能が得られて来ている。

尖った電子密度の分布が改善されたLモード(ILモード)プラズマで測定され、それはHモード領域で観測されたものと対照的である。ペレット注入時、同様に尖った密度分布が観測された。

Contents

1. Introduction	1
2. Thomson Scattering System	2
3. Fiber Bundle Construction	4
4. Profile Measurements	5
5. Summary	6
Acknowledgements	6
References	7

目 次

1. 緒 言	1
2. トムソン散乱装置	2
3. バンドル・ファイバーの構成	4
4. 分布測定	5
5. 総 論	6
謝 辞	6
参考文献	7

1. Introduction

Several tokamak experiments have been equipped with multi-point Thomson scattering systems [1-8]. A TV Thomson scattering system (TVTS) has been developed at the Princeton Plasma Physics Laboratory (PPPL) and installed on PLT, PBX and TFTR [1-3], as well as on DIII and DIII-D [4,5]. A light detection and ranging (LIDAR) system has been developed for the Joint European Torus (JET) [6]. The spatial resolution of the former system is about 1cm and that of the latter about 10cm. In order to obtain the temporal evolution of the profiles, further development of the TVTS would be required. One complete profile is usually obtained with each tokamak discharge, except in the case of scattering systems using YAG lasers [7]. For a small tokamak like JFT-2M, a TVTS system would be suitable for measuring electron temperature and density profiles.

On JFT-2M, a 13-point Thomson scattering system using photomultiplier (PM) detection has been taking data for 2 years [9]. Although measurements are presently being made at 13 spatial positions, this number could be increased to 38 or more. The present configuration represents a compromise as concerns the physical size of the enclosure containing the PM tubes. The separation in the plasma between adjacent measuring points is approximately 5cm.

PM tubes have been chosen because of their wide dynamic range, high gain, high quantum efficiency and highly-reproducible gating action during data acquisition. Because of variations in quantum efficiency over the surface of the photocathodes, as well as sample-to sample variations in the tubes themselves, careful calibration of each tube is necessary in order to obtain accurate data. Rather than a tungsten-filament lamp, LED's have been used for this calibration [10].

This paper describes the components of the 13-point Thomson scattering system, with emphasis on the glass fiber optic bundle. Electron temperature (T_e) and density (n_e) profiles for plasmas showing good confinement (improved L-mode and other modes) are also presented and discussed.

2. Thomson Scattering System

The Thomson scattering system described here, shown in Fig.1, represents an upgrade of a 6-point system described previously [8]. A typical optical path is shown in Fig.2. The collecting lens is designed for gathering light from a 110cm long vertical plasma volume. The lens is of Gaussian type, as was also the case in the previous design. Vignetting from the observation window limits the vertical field of view to a length of 60cm. The optical axis of the lens is 10cm below the plasma mid-plane. A motor-driven vertical adjustment of 5cm is provided. The diameter of the collecting lens is approximately twice that of the 6-point Thomson scattering system [8]. The lowest observation point in the plasma(position 1) is 10cm below the plasma mid-plane, for which the scattering angle is 80° . The scattering angle for the highest observation point, at position 13, is 131° . The spatial resolution is 1.6cm at the plasma mid-plane. A polarizer plate mounted behind the collecting lens reduces plasma radiation and stray light by half. Each fiber bundle is mounted with its input face perpendicular to the optical axis. The fiber bundles depolarize the scattered light. This effect simplifies the calibration procedure by removing the differences in polarization between the scattered light and the unpolarized LED radiation used for calibration. (The reflectivities of the diffraction grating and of other optical surfaces in the beam path are polarization-dependent.) High-pass optical filters are mounted at the input end of the first optical fiber bundle in order to decrease the stray light. The output end of the fiber bundle is divided into 2 sections, each going to the input slit of a separate spectrometer. The spectrometers are again of the Littrow type, but with a larger wavelength range:5200-7000Å. A second fiber bundle runs from the output slits of each spectrometer to the PM tubes(48 in all). The optical transmission of the system is similar to that of the previous one. The PM tubes are gated on for 3-8 sec for detection of scattered light, and again after 10 sec for the same time interval in order to measure the plasma light. The output signals are amplified tenfold and then attenuated as required to accommodate the dynamic range of 500 counts of the

A/D converter. The attenuation is adjusted from the control room, the attenuation values and the scattered signals being recorded together. The signals are integrated during the 100nsec gate duration. Graphic display of electron temperature and density profiles follows immediately. In addition, untreated data is stored in a memory module in the CAMAC crate for subsequent transfer to the central computer(Mitsubishi Ltd [11]). Software has been developed for calculating T_e and n_e from the experimental data [10]. Automatic recording and display of the 180 attenuation values increases system reliability.

The Q-switched laser system [8], producing about 4J, has been in operation since 1977.

3. Fiber Bundle Construction

Recent improvements in the reliability of optical fibers have motivated their use between the collecting lens and the spectrometers, and also at the output of each spectrometer. This modification has reduced the optical path between the collecting lens and the spectrometers from about 2m to less than 1m, thus reducing the size of the optical system. Figure 2 shows a typical path through the complete optical system. When a large lens with a large solid angle is used for collecting scattered light, correct matching requires the use of a fiber of small numerical aperture. The field lens transmits light from the fiber bundle to the Littrow lenses in each of the two spectrometers used for analyzing the radiation scattered from the 13 vertically-arranged points. Here a flexible fiber bundle is used, in contrast to the systems developed for PLT and DIII-D, where small-diameter (50 micron) flexible glass fibers are used. The flexible type used here allows easy modification of measuring positions and spectral channels by interchanging fibers or moving the collecting lens vertically. Except for the number of channels, the fiber bundles used here are similar to those previously employed. Each bundle in the first has an input end of rectangular cross-section, while two output faces are curved, with dimensions 70mm by 3mm. The dimensions of height is larger than that of the bundle used previously [8]. The 13 measuring points are separated into 2 groups for spectral analysis—the 7 points from the central (high temperature) region, and the 6 from the edge (low temperature) region. In order to reduce losses, the fibers are kept as short as possible.

4. Profile Measurements

Density calibration is performed using Raman scattering and the spectral calibration is performed using LED's [12]. The average electron density determined from Thomson scattering correlates well with values obtained from HCN interferometer measurements, as shown in Fig.3.

Profiles obtained during the H-mode phase have already been presented previously [13,14]. Here we present profiles obtained during the improved L-mode(IL-mode) phase. The IL-mode plasma is described elsewhere [15]. The global plasma energy is higher than in the H-mode, as shown in Fig.4. Their profiles are shown in Fig.5(a) and (b), the latter showing the peaked profiles observed during the IL-mode phase. The edge electron density decreases by about 50% through the disappearance of the electron temperature pedestal which is the resulting increase in the diffusion coefficient $D=0.2 \times x_e$, as derived from the relation $x_e = \text{const}/(n_e \cdot dT_e/dr)$. A steepened gradient is measured during the early phase of the H-mode, while the L-mode phase is characterized by greater decay lengths of profiles at the plasma edge for both the electron density and the plasma emission [16].

The peaking ratio of electron density, $n_{e0}/\langle n_e \rangle$, n_{e0} and $\langle n_e \rangle$ being the central electron density and the volume-averaged value of electron density respectively, is high in the IL-mode phase, as shown in Fig.6. The IL-mode can be characterized by a specific electron behavior, namely a larger value of T_e due to the peaked, narrow n_e profile. Such conditions are favorable for central energy deposition using neutral beam injection to produce a high and broad electron temperature profiles. We next present results obtained during pellet injection. In many discharges, pellet injection causes profile changes. Higher central density and peaked profile, as shown in Fig.7, results. n_e profile is similar to those of the IL-mode phase.

5. Summary

A 13-point Thomson scattering system for measuring T_e and n_e has been collecting data reproducibly since 1987. The following points should be noted.

- 1) A large collecting lens collects the light scattered from a 60cm long plasma volume.
- 2) Attenuation values from 180-channel attenuator are automatically transferred into the CPU memory.
- 3) High-pass optical filters and polarizer plate are used to reduce stray light.
- 4) The fiber bundles used minimize the polarization differences between the scattered light and that used for calibration.
- 5) The system operates reliably for electron densities above $(4-5) \times 10^{12} \text{cm}^{-3}$.
- 6) Peaked density profiles are measured in the IL-mode, in contrast to those of the H-mode.
- 7) Broad temperature profiles are measured in the IL-mode, which will lead to good confined plasmas.
- 8) The electron energy in the IL-mode is higher than in the H-mode, due to the increase of electron temperature.
- 9) The density peaking ratio is highest in the IL-mode, which is similar to that of pellet injection.

Acknowledgements

I would like to thank Mr.K.Suzuki and his group for their operation of JFT-2M. I am grateful to Dr.H.Aikawa for useful discussions. I would also like to express our gratitude to Drs.H.Maeda, S.Shimamoto, M.Tanaka, M.Yoshikawa and S.Mori for their continual encouragement.

References

- [1]N.Bretz et al., Appl. Opt. 17 (1978) 192.
- [2]D.Johnson et al., Rev. Sci. Instrum. 57 (1986) 1810.
- [3]D.Johnson et al., Rev. Sci. Instrum. 57 (1986) 1856.
- [4]D.Vaslow, General Atom. Rep. GA-A16378(1981)
- [5]C.L.Hsieh et al., General Atom. Rep. GA-A19192 (1988).
- [6]H.Salzmann et al., Joint Eur. Tok. Rep. JET-P(87)16 (1987).
- [7]H.Rohr et al., Max Planck Inst.Rep. IPP III/121 B (1987).
- [8]T.Yamauchi et al., Japan J. Appl. Phys. 21 (1982) 347.
- [9]T.Yamauchi et al., Japan At.Energ. Res. Inst. Rep. JAERI-M 87-196 (1987).
- [10]T.Yamauchi and I.Yanagisawa, Japan J. Appl. Phys. 25 (1986) 263.
- [11]T.Matsuda et al., Japan At. Energ. Res. Inst. Rep. JAERI-M 87-129 (1987).
- [12]T.Yamauchi and I.Yanagisawa, Appl.Opt. 24 (1985) 700.
- [13]T.Yamauchi et al., Phys. Lett. A 131 (1988) 301.
- [14]T.Yamauchi and JFT-2M Group, Japan J. Appl. Phys. 27 (1988) L924.
- [15]M.Mori et al., Nucl. Fusion Lett. 28 (1988) 1891.
- [16]T.Yamauchi and JFT-2M Group, Japan J. Appl. Phys. 28 (1989) L365.

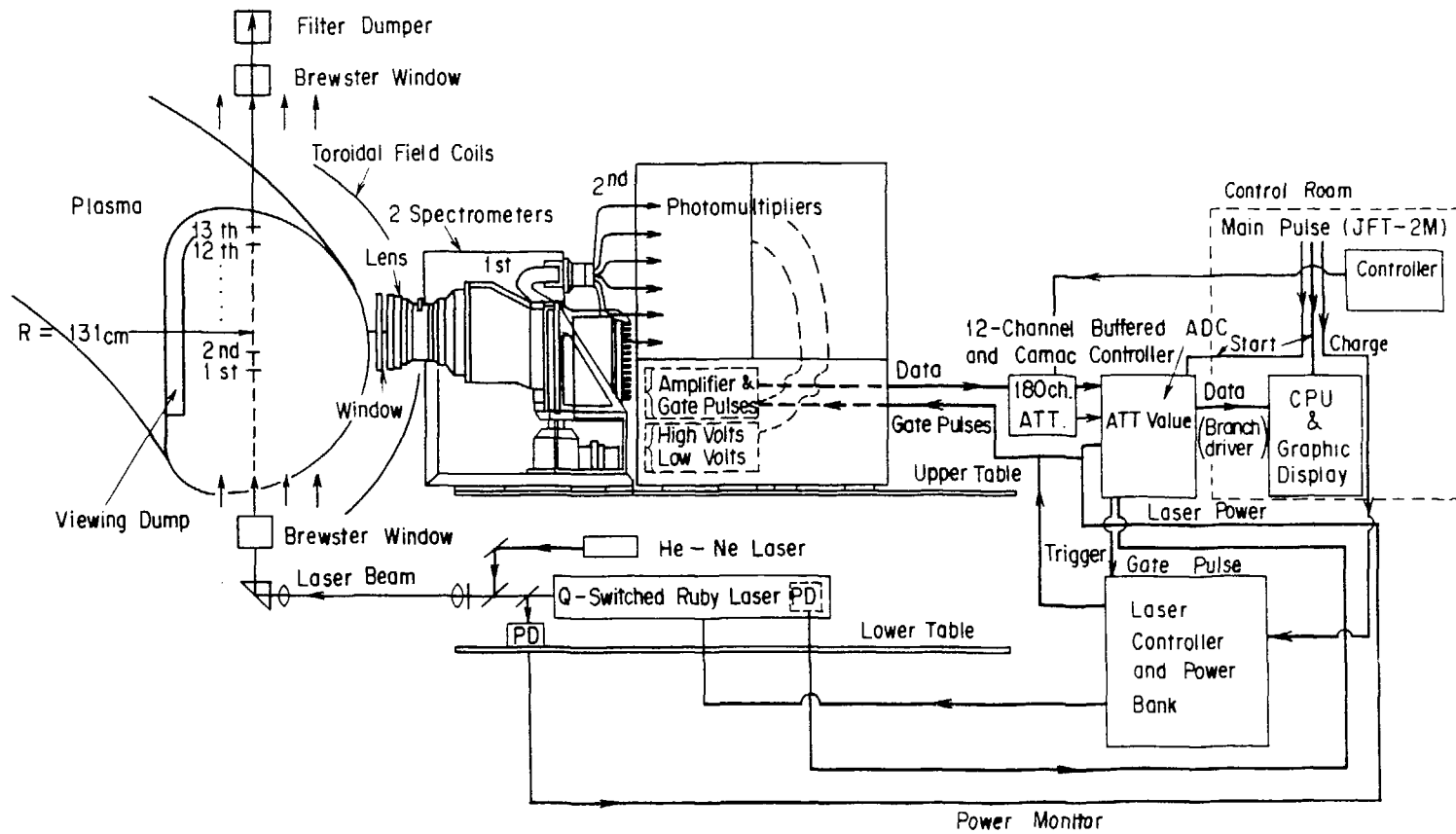


Fig. 1 Physical arrangement of laser, JFT-2M tokamak plasma, spectrometers and central processing unit (CPU).

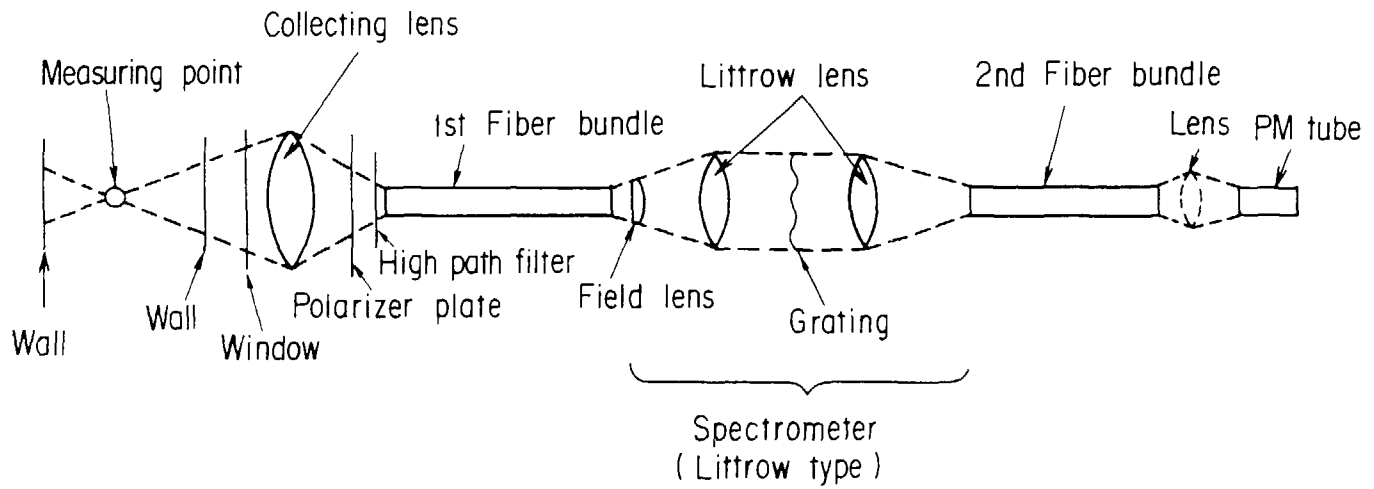


Fig. 2 Optical path of the 13-point Thomson scattering system.

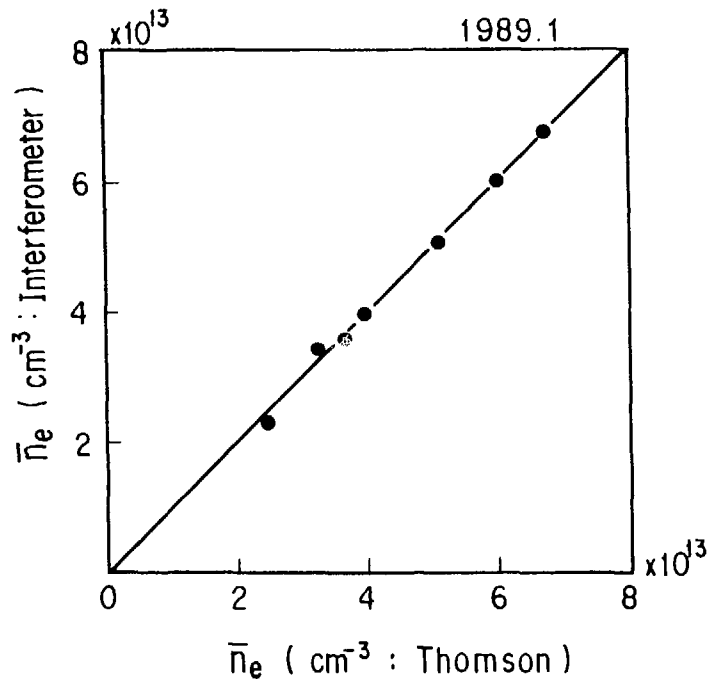


Fig. 3 Comparison of average electron density obtained from Thomson scattering and from HCN-laser interferometer measurements.

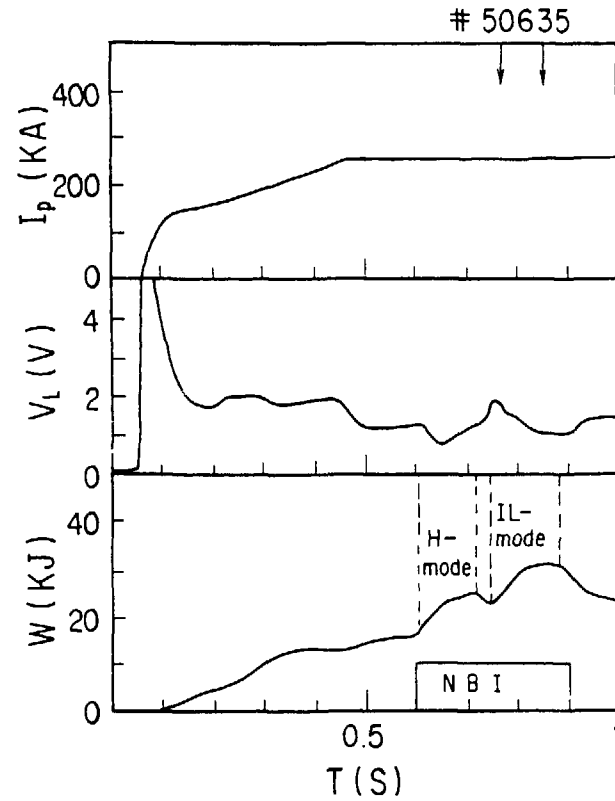


Fig. 4 Time evolution of plasma current, I_p , loop voltage, V_L , and global energy, W for a He⁺⁺ plasma. $P_{nbi} = 0.36$ MW (He beam), $B_t = 1.34$ T, $I_p = 250$ kA, lower single-null divertor configuration.

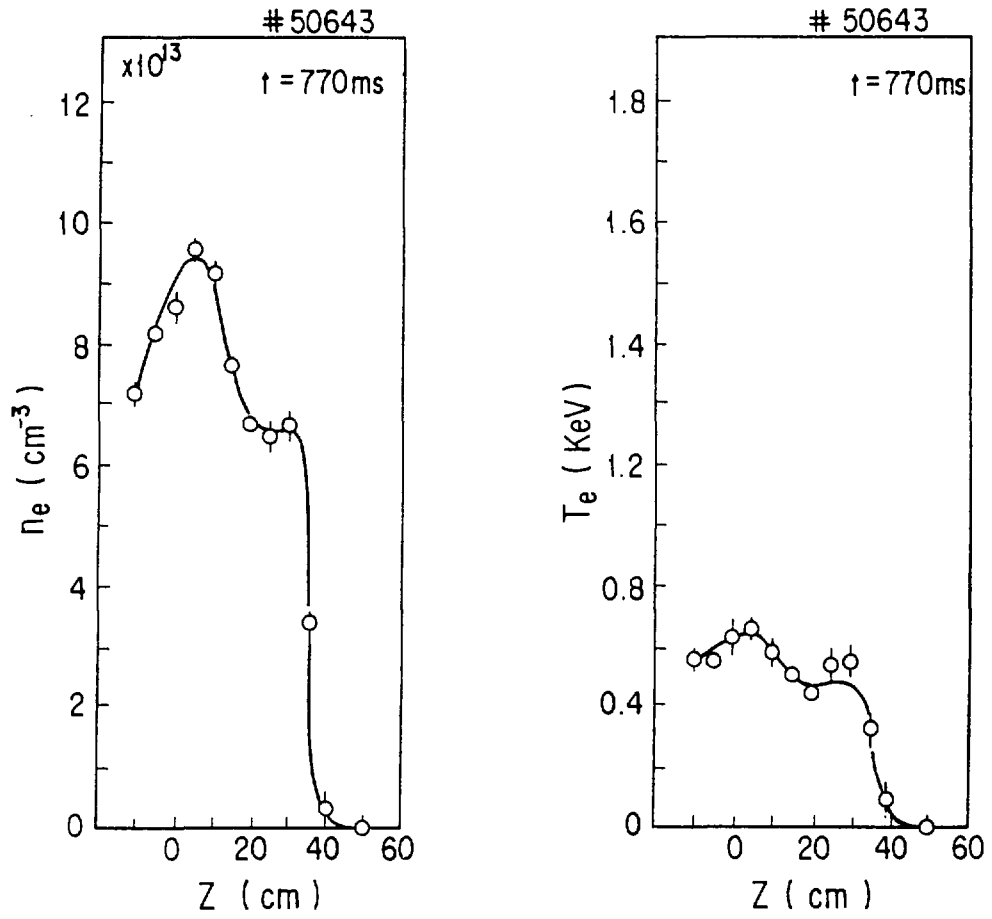


Fig. 5 (a) Electron density and temperature profiles in the H-mode phase.

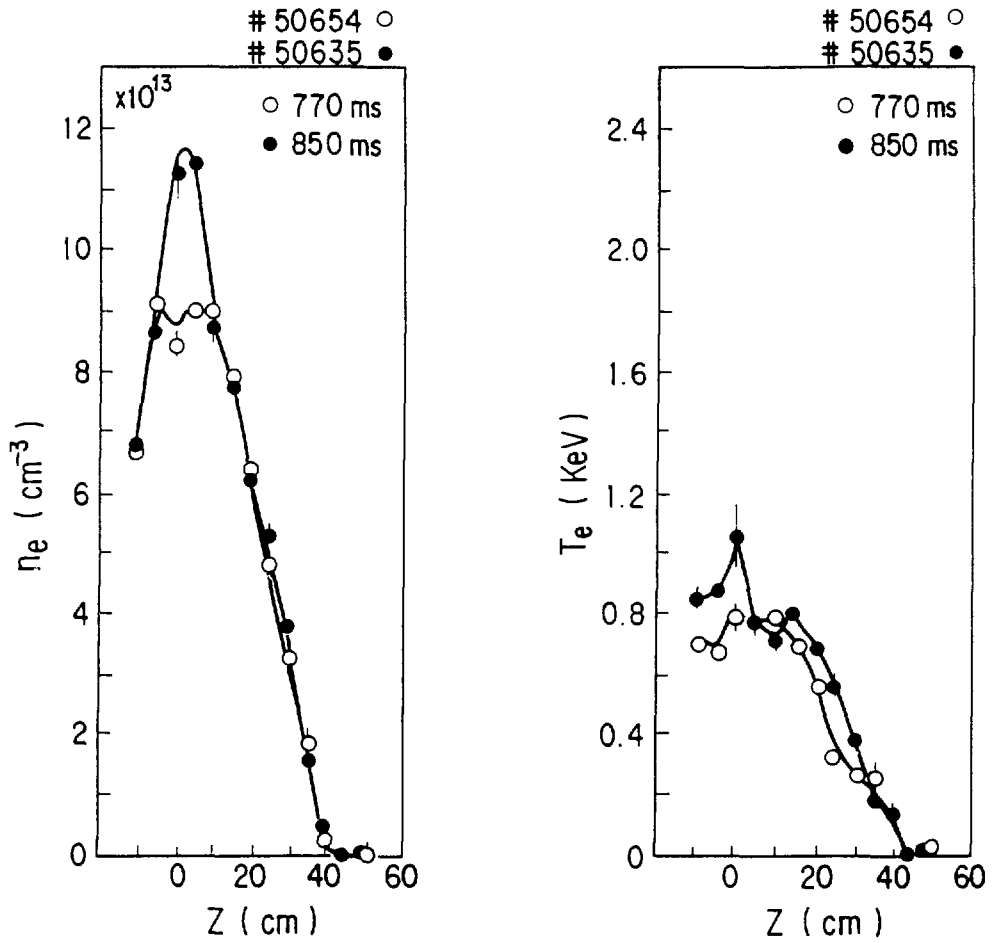


Fig. 5 (b) Electron density and temperature profiles in the IL-mode phase.

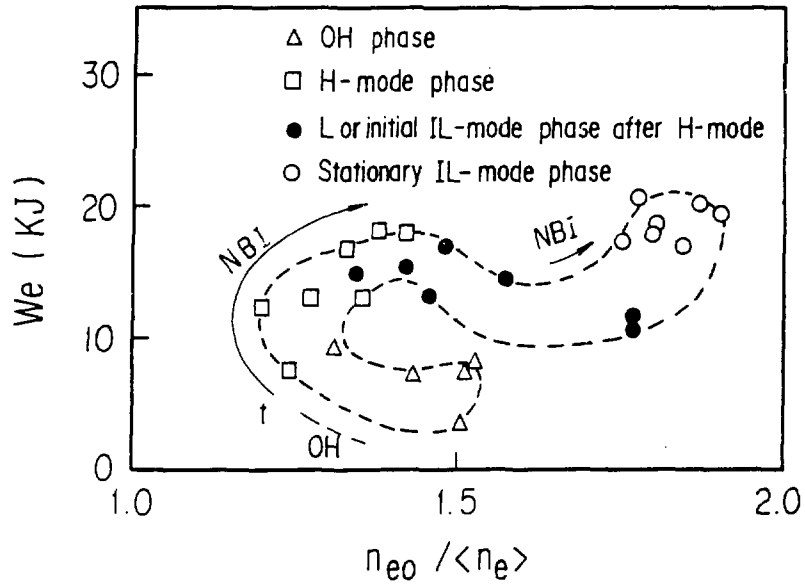


Fig. 6 Electron energy as a function of electron density peaking ratio, $n_{e0} / \langle n_e \rangle$.

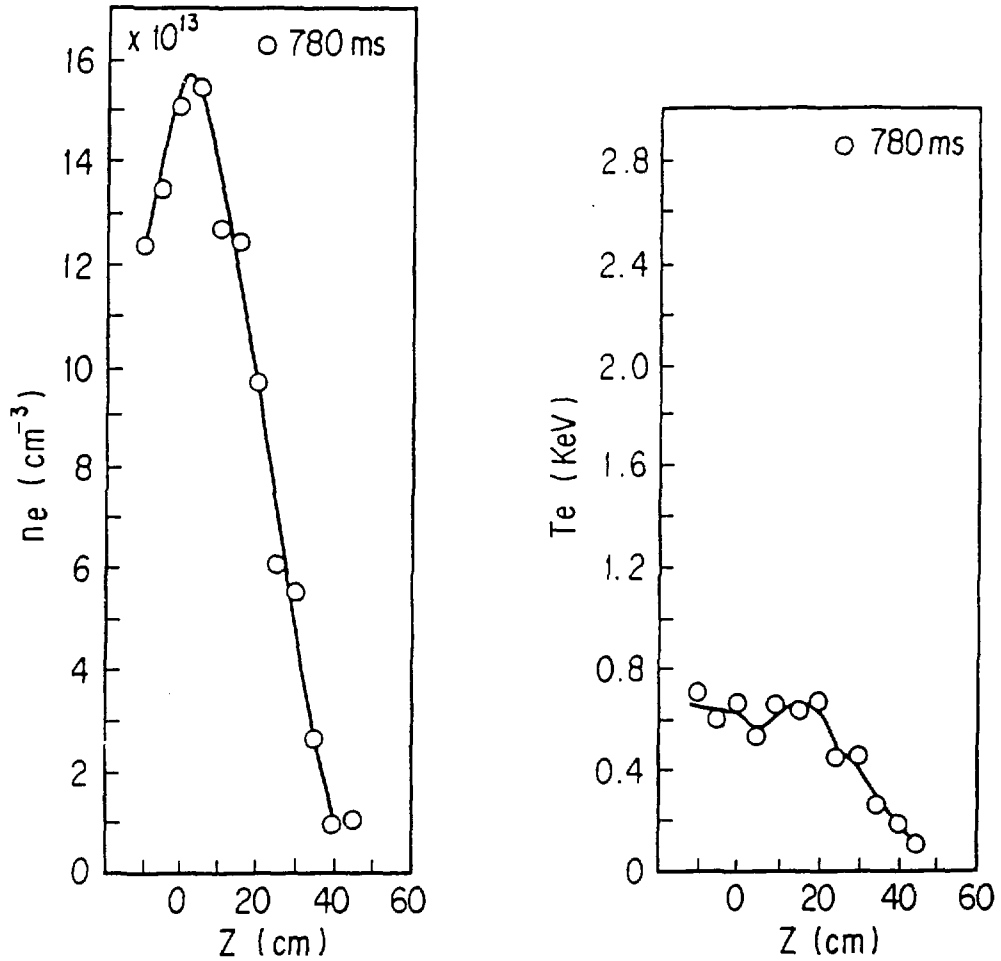


Fig. 7 Electron density and temperature profiles during pellet injection, $P_{\text{NBI}} = 0.8 \text{ MW}$ (from 700ms), $B_t = 1.34 \text{ T}$, $I_p = 290 \text{ kA}$, D^+ plasma, three deuterium pellets and lower single-null divertor configuration.